

# A Direct Spectral Domain Method for Near-ground Microwave Radiation by a Vertical Dipole above Earth in the Presence of Atmospheric Refractivity

R. Bhattacharjee<sup>1,2</sup>, C. R. Anderson<sup>2</sup>, and G. D. Durgin<sup>1</sup>

<sup>1</sup>Georgia Institute of Technology, USA

<sup>2</sup>United States Naval Academy, USA

**Abstract**— A spectral domain method is presented to calculate the potential of a vertical dipole in a multilayered medium as a model of long-range radio propagation. The spectral domain Green's function (SDGF) for structures with up to hundreds of thousands of layers is calculated using an efficient matrix formulation, thus enabling simulation of continuously stratified media. The SDGF is sampled to perform pole/residue-extraction using contour quadratures and to perform a novel asymptotic Filon-Clenshaw-Curtis (FCC) quadrature to calculate the far-field Green's functions. The near-fields are directly calculated using an adaptive Clenshaw-Curtis quadrature without pole-extraction. Results of numerical simulations are presented in the case of a graded-index waveguide and an atmospheric gradient-layer above a realistic lossy ground.

## 1. INTRODUCTION

Electromagnetic (EM) modeling of refractive and terrain effects over long links has been modeled by ray tracing [1, 17, 20] or by using the parabolic/paraxial wave equation [3, 4, 7]. These methods are approximations to the wave propagation physics of Maxwell's equations, which can limit their applicability. Other approaches have included the moving-window finite-difference time-domain (MWFDTD) method [14, 16, 21, 22]. While capturing the relevant physics, MWFDTD leaves something to be desired with respect to intuition about the fields; a list of field strength values is not readily understood in terms of propagation mechanisms such as direct waves, reflected waves, interface/ground waves, and guided propagation modes.

On the other hand, the theory of Sommerfeld integrals (SIs) and spectral domain Green's functions (SDGFs) in multilayered media has been used in the simulation of printed circuit board (PCB) structures such as transmission lines and antennas [8]. The SDGF/SI technique expresses the EM fields as SIs, which must be evaluated numerically using a variety of methods [2, 13, 15, 18]. With certain approaches, the solutions decompose into terms that directly correspond to the aforementioned propagation mechanisms. The key contribution of the present work is the application of these rigorous full-wave techniques to long range radio frequency (RF) propagation. Quadrature methods used for PCBs are not directly applicable because of the differences in length scales involved. We therefore use novel asymptotic quadrature to calculate far-fields, an approach that has not, to the best of our knowledge, been attempted for RF propagation before.

## 2. ATMOSPHERIC AND EM MODEL

The problem geometry is a non-magnetic, multilayered dielectric material bounded by two half-spaces with interfaces parallel to the  $xy$ -plane that contains a  $z$ -directed, time harmonic ( $e^{-j\omega t}$  time dependence) dipole radiator at a height  $z'$  above the origin, as in Figure 1. Each layer is homogeneous with index of refraction  $n_\ell = \sqrt{\varepsilon_0 \varepsilon_{r\ell}}$ , where  $\varepsilon_{r\ell}$  is the relative permittivity of the  $\ell^{\text{th}}$  medium and  $\varepsilon_0 \approx 8.85418782 \times 10^{-12}$  F/m is the permittivity of free space. The media wavenumbers are  $k_\ell = n_\ell k_0$ ,  $k_0 = 2\pi f/c_0$ ,  $f$  is the frequency of the wave, and  $c_0 = 299,792,458$  m/s is the speed of light in vacuum. The EM fields in this geometry can be expressed in terms of only the  $z$  component of the magnetic vector potential,  $A_z(\rho, z, z')$ , where  $\rho$  is the  $xy$ -distance away from the dipole and  $z$  is the height above the origin.  $A_z$  obeys a forced wave-equation in the source layer, and an unforced one in the others. The equation reduces to the 3D Helmholtz equation under harmonic time dependence, which is indicated in Figure 1.

The spatial domain potential can be shown to admit a spectral (Sommerfeld) integral representation given by

$$A_z(\rho, z, z') = \int_0^\infty \tilde{A}_z(k_\rho, z, z') J_0(k_\rho \rho) k_\rho dk_\rho, \quad (1)$$

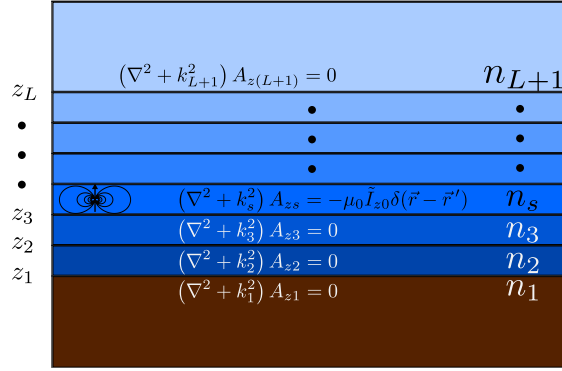


Figure 1: A dipole radiates inside layers of dielectric material. There are  $L$  layer interfaces, and  $L + 1$  layers including the top and bottom semi-infinite half-spaces.

where  $J_0$  is the Bessel function of the first kind and order zero and  $k_\rho$  is the radial wavenumber of a spectral component. The SDGF  $\tilde{A}_z$  is split in a piecewise manner into functions in each layer, noted as  $\tilde{A}_{z\ell}$  for  $\ell = 1, 2, \dots, L + 1$ . These functions obey a 1D Helmholtz equation in each layer,

$$\frac{\partial^2 \tilde{A}_{z\ell}}{\partial z^2} + k_{z\ell}^2 \tilde{A}_{z\ell} = \begin{cases} -\mu_0 \tilde{I}_{z0} \frac{\delta(z-z')}{4\pi^2}, & \text{in source layer} \\ 0, & \text{in other layers,} \end{cases} \quad (2)$$

where  $\tilde{I}_{z0}$  is the complex magnitude of the current flowing in the dipole,  $\mu_0 = 4\pi \times 10^{-7}$  H/m is the permeability of free space, and in each layer the  $z$  wavenumber is given by the auxiliary relationship  $k_{z\ell} = \sqrt{k_\ell^2 - k_\rho^2}$ . Equation (2) is to be solved in all layers simultaneously for a given  $k_\rho$ . Then Equation (1) is calculated by numerical quadrature over various values of  $k_\rho$ .

### 3. SPECTRAL DOMAIN GREEN'S FUNCTION SOLVER

The general solution to Equation (2) is

$$\tilde{A}_{z\ell} = j \frac{\mu_0 \tilde{I}_{z0}}{8\pi^2} \times \begin{cases} \frac{e^{jk_{z\ell}|z-z'|}}{k_{z\ell}} + R_\ell^+ e^{jk_{z\ell}(z-z_{\ell-1})} + R_\ell^- e^{-jk_{z\ell}(z-z_\ell)}, & \text{in source layer} \\ R_\ell^+ e^{jk_{z\ell}(z-z_{\ell-1})} + R_\ell^- e^{-jk_{z\ell}(z-z_\ell)}, & \text{in other layers,} \end{cases} \quad (3)$$

where  $R_\ell^\pm$  are generalized reflection coefficients in each layer that have to be fixed by boundary conditions. The boundary conditions are that the tangential EM fields have to be continuous at the layer interfaces, and that there are no incoming waves ( $R_1^+ = R_{L+1}^- = 0$ , the Sommerfeld radiation condition). Applying these to Equation (3) reduces the problem to a linear system of equations for the  $R_\ell^\pm$  coefficients, the exact details of which are to follow in a future publication. The system of equations is sparse: each equation involves only four of the  $2L$  unknowns. The sparse system can be assembled into a  $2L \times 2L$  pentadiagonal matrix with at most  $(10L - 6)$  nonzero entries out of the full  $4L^2$ . The memory requirements for large numbers of layers in the structure are not prohibitive. Optimized algorithms exist for solving pentadiagonal systems; this leads to  $O(L)$  time-complexity for solving for  $R_\ell^\pm$ . At the time of writing, a typical computer can solve systems of  $L \sim 100,000$  layers in  $\sim 1$  second. Once the matrix equation is solved for the  $R_\ell^\pm$ , the SDGF can be evaluated at arbitrary heights  $z$  using Equation (3). The matrix is formed and solved, and the SDGF is evaluated at multiple heights each time the quadrature routines of the next section require samples from the SDGF, which happens during both pole-extraction and asymptotic quadrature.

### 4. QUADRATURE OF THE SPECTRAL DOMAIN GREEN'S FUNCTIONS

SIs are considered to be difficult to numerically integrate due to their slow decay and oscillations [2, 12, 13, 15, 24]. The slow decay is from poles on or near the real  $k_\rho$ -axis in the SDGF, which degrade the ability of numerical integration algorithms to converge. The oscillations are from the the Bessel function  $J_0(k_\rho \rho)$ , which oscillates more rapidly as  $\rho$  increases. Conventional quadratures

have to calculate *more* points from the integrand/SDGF as the range increases to resolve the details of the Bessel function. Far-field calculations are therefore time-consuming and intensive. In this work, the slow decay and rapid oscillation problems are handled using two separate techniques, one well established, and the other novel.

#### 4.1. Handling Slow-decay with Pole Extraction

Poles and residues are extracted from the SDGF and analytically integrated using the residue theorem. An effective search algorithm based on complex contour integrals, which automatically finds the pole wavenumbers and residues, has been described in the literature [9, 13]. In the present work, the poles are located by refining user-provided initial guesses with a direct search optimization and *then* contour integrals are used to calculate residues. These are approximated by an adaptive Gauss-Kronrod quadrature adapted from [19, 23]. The residues at all desired heights are calculated in parallel by the chosen Gauss-Kronrod algorithm. The poles are known to come in opposing pairs,  $\pm k_p$ , so the residue theorem is applied to SIs of the form  $\int_0^\infty \frac{1}{k_\rho^2 - k_p^2} J_0(k_\rho \rho) k_\rho dk_\rho = \frac{j\pi}{2} H_0^{(1)}(k_p \rho)$ , where the pole is at  $k_\rho = k_p$ , and  $H_0^{(1)}$  is the Hankel function of the first kind and order zero.

#### 4.2. Handling Oscillatory Integrands with Filon-like Asymptotic Quadratures

The standard approach to quadrature of oscillatory integrands is to sample them on enough points to resolve the oscillations and then approximate the integral as a weighted sum of the sampled values. For the present case this would mean that the number of SDGF samples would increase in proportion to the range  $\rho$ . Calculation of far-fields would require *more* computational effort than the near-fields. However, there are several families of *asymptotic* quadratures that *increase* in accuracy as the oscillation increases [10, 11]. The method used presently is the Filon-Clenshaw-Curtis (FCC) rule [5, 6]. Although designed for complex exponential oscillation, far-field SIs can be adapted for the FCC in the following way. Since we're interested in asymptotic results, the Bessel function is replaced by its asymptotic expansion in Equation (1), giving

$$A_z(\rho, z, z') \approx \sqrt{\frac{1}{2\pi\rho}} \int_0^\infty \tilde{A}_z(k_\rho, z, z') \left( e^{jk_\rho \rho - j\frac{\pi}{4}} + e^{-jk_\rho \rho + j\frac{\pi}{4}} \right) \sqrt{k_\rho} dk_\rho, \quad (4)$$

which can be broken up into two integrals, each of which has a form that is directly amenable to FCC quadrature after the semi-infinite interval is truncated to a large finite value. Finite truncation is justified physically because the pole-extracted SDGF decays exponentially beyond the largest material wavenumber and the rapid spatial oscillations of large wavenumbers are known to contribute only to the near-field singularity; the corresponding waves do not propagate into the far-field.

## 5. NUMERICAL EXPERIMENTS

The method presented is general, and could be applied to any multilayered problem. As a proof-of-concept, consider a PCB-type example in which a copper substrate has a graded-index material coated on it, with a linear gradation of 10% over ten wavelengths. A plot of the extracted guided mode potentials as a function of height and range appears in the top panel of Figure 2. There are seven poles corresponding to guided propagation in the structure. It is clear from the plots that the structure acts as a waveguide, trapping the energy in the refractive gradient. In this example, the source dipole is 3.1123 wavelengths above the substrate. The lower panel of Figure 2 is a plot of ray paths that propagate in the same gradient over a reflective ground plane. The two plots compare favorably in terms of the distance scale of the modal “skip zones.”

Another numerical example appears in Figure 3, with the top panel representing a dipole radiating above earth with  $\epsilon_r = 15$  and a conductivity of  $\sigma = 12 \times 10^{-3}$  S/m in a strong gradient, with  $n(z) = 1 + e^{-z}/10$  above ground. While this is an unusually strong gradient for atmospheric cases, it is an exaggerated example to illustrate the effects of propagation through refractive gradients at ranges that can be easily visualized. For more realistic gradients, the effects are apparent farther away from the dipole. Because the FCC quadrature becomes more accurate farther away, and there is no additional computational cost of increasing range, there is no inherent problem with calculating extremely far fields, only one of visualizing the long length scales in the kinds of plots presented. Log-scaled line plots can be appropriate, but we find the visualization of the figures presented more illustrative. The visualized potential is calculated by the sum of guided modes and the asymptotic FCC quadrature result for  $\rho > 20\lambda_0$  and by a direct Clenshaw-Curtis quadrature for  $\rho \leq 20\lambda_0$ . The

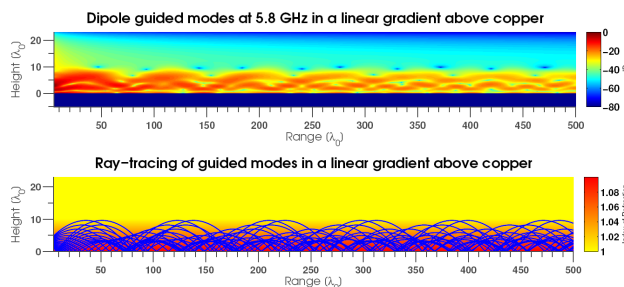


Figure 2: A dipole radiates in a layered coating on a copper substrate at 5.8 GHz. The potential  $A_z(\rho, z)$  is visualized on a decibel scale.

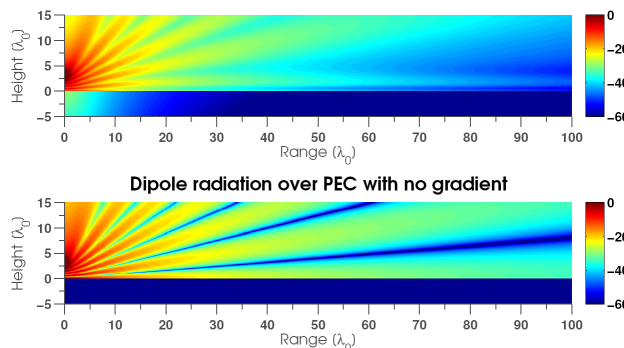


Figure 3: A dipole radiates in two similar scenarios. The top panel is using the SDGF/SI method in an actual scenario and the bottom panel is using image theory in an idealized scenario.

fact that there is no discernible discontinuity in the fields at  $\rho = 20\lambda_0$  is evidence of the accuracy of the far-field approximation and FCC quadrature. The lower panel of Figure 3 is a comparison with a simplified environmental model that can be solved using image-theory, a technique that is widely used by communications engineers as the “two-ray” model. The differences between the two are apparent at the surface level, where the two-ray model can be said to break-down.

## 6. CONCLUSION

A direct method for calculating EM fields in multilayered media based on SDGFs and quadrature of SIs has been presented. Application of asymptotic quadratures to SI problems is novel to our knowledge. Although the technique is conceived of as a method for simulating long range radio propagation near ground level, it is applicable to general EM propagation in multilayered media. Initial testing indicates agreement with the physics; indeed, the calculated fields do solve Maxwell’s equations and boundary conditions. Future directions include careful validation against other models and measurements, exploring enhancements to speed convergence, formulating the solution for horizontal dipoles, and finally handling terrain through boundary-integral/scattering methods.

## ACKNOWLEDGMENT

We’d like to thank Dr. Víctor Domínguez for his work on the FCC quadrature and willingness to answer questions via email. This work was funded by the Office of Naval Research.

## REFERENCES

1. Akbarpour, R. and A. R. Webster, “Ray-tracing and parabolic equation methods in the modeling of a tropospheric microwave link,” *IEEE Transactions on Antennas and Propagation*, Vol. 53, No. 11, 3785–3791, 2005.
2. Aksun, M. and G. Dural, “Clarification of issues on the closed-form Green’s functions in stratified media,” *IEEE Transactions on Antennas and Propagation*, Vol. 53, No. 11, 3644–3653, 2005.
3. Dockery, G., R. Awadallah, D. Freund, J. Gehman, and M. Newkirk, “An overview of recent advances for the TEMPER radar propagation model,” *2007 IEEE Radar Conference*, 896–905, Apr. 2007.

4. Dockery, G. D., “Modeling electromagnetic wave propagation in the troposphere using the parabolic equation,” *IEEE Transactions on Antennas and Propagation*, Vol. 36, No. 10, 1464–1470, Oct. 1988.
5. Domínguez, V., I. Graham, and T. Kim, “Filon-Clenshaw-Curtis rules for highly-oscillatory integrals with algebraic singularities and stationary points,” *SIAM Journal of Numerical Analysis*, 2013, to Appear.
6. Domínguez, V., I. G. Graham, and V. P. Smyshlyaev, “Stability and error estimates for Filon-Clenshaw-Curtis rules for highly oscillatory integrals,” *IMA Journal of Numerical Analysis*, Vol. 31, No. 4, 1253–1280, 2011.
7. Donohue, D. and J. Kuttler, “Propagation modeling over terrain using the parabolic wave equation,” *IEEE Transactions on Antennas and Propagation*, Vol. 48, No. 2, 260–277, Feb. 2000.
8. Fang, D. G., *Antenna Theory and Microstrip Antennas*, CRC Press, 2010.
9. Hu, B. and W. C. Chew, “Fast inhomogeneous plane wave algorithm for electromagnetic solutions in layered medium structures: Two-dimensional case,” *Radio Science*, Vol. 35, No. 1, 31–43, 2000.
10. Iserles, A. and S. Nøsett, “On quadrature methods for highly oscillatory integrals and their implementation,” *BIT Numerical Mathematics*, Vol. 44, No. 4, 755–772, 2004.
11. Iserles, A., S. Nøsett, and S. Olver, “Highly oscillatory quadrature: The story so far,” *Numerical Mathematics and Advanced Applications*, A. de Castro, D. Gómez, P. Quintela, and P. Salgado, Eds., 97–118, Springer Berlin Heidelberg, 2006.
12. Kaifas, T., “Direct rational function fitting method for accurate evaluation of sommerfeld integrals in stratified media,” *IEEE Transactions on Antennas and Propagation*, Vol. 60, No. 1, 282–291, 2012.
13. Ling, F. and J.-M. Jin, “Discrete complex image method for Green’s functions of general multilayer media,” *IEEE Microwave and Guided Wave Letters*, Vol. 10, No. 10, 400–402, 2000.
14. Luebbers, R., J. Schuster, and K. Wu, “Full wave propagation model based on moving window FDTD,” *2003 IEEE Military Communications Conference, MILCOM’03*, Vol. 2, 1397–1401, 2003.
15. Michalski, K., “Extrapolation methods for Sommerfeld integral tails,” *IEEE Transactions on Antennas and Propagation*, Vol. 46, No. 10, 1405–1418, 1998.
16. Ohs, R. R., J. W. Schuster, and T. Y. Fung, “Full wave simulation of radiowave propagation in unattended ground sensor networks,” *Proc. IEEE Radio and Wireless Symp. RWS’09*, 183–186, 2009.
17. Ozgun, O., “Recursive two-way parabolic equation approach for modeling terrain effects in tropospheric propagation,” *IEEE Transactions on Antennas and Propagation*, Vol. 57, No. 9, 2706–2714, Sep. 2009.
18. Quinto, M., S. Boutami, and J. Hazart, “Fast computation of dipole radiation in stratified background using graphics processing unit,” *Progress In Electromagnetics Research M*, Vol. 20, 115–126, 2011.
19. Shampine, L. F., “Vectorized adaptive quadrature in MATLAB,” *J. Comput. Appl. Math.*, Vol. 211, No. 2, 131–140, Jan. 2008.
20. Valtr, P. and P. Pechac, “Analytic tropospheric ray-tracing model for constant refractivity gradient profiles,” *First European Conference on Antennas and Propagation, EuCAP 2006*, 1–4, 2006.
21. Wu, K., J. Schuster, and R. Luebbers, “Full wave modeling of RF propagation between low-to-the-ground antennas,” *2005 IEEE Antennas and Propagation Society International Symposium*, Vol. 2B, 711–714, 2005.
22. Wu, K., J. Schuster, R. Ohs, and R. Luebbers, “Application of moving window FDTD to modeling the effects of atmospheric variations and foliage on radio wave propagation over terrain,” *2004 IEEE Military Communications Conference, MILCOM 2004*, Vol. 3, 1515–1521, 2004.
23. Wyatt, A., QUADVGK: Vectorised adaptive G7,K15 Gaussian quadrature on vector of integrals, Feb. 2008.
24. Yuan, M., T. Sarkar, and M. Salazar-Palma, “A direct discrete complex image method from the closed-form Green’s functions in multilayered media,” *IEEE Transactions on Microwave Theory and Techniques*, Vol. 54, No. 3, 1025–1032, 2006.